

Reversible waveform conversion between microwave and optical fields in a hybrid opto-electromechanical system_

Li-Guo Qin(秦立国), Zhong-Yang Wang(王中阳), Jie-Hui Huang(黄接辉),Li-Jun Tian(田立君), and Shang-Qing Gong(龚尚庆)

Citation: Chin. Phys. B, 2021, 30 (**6**): 068502. DOI: 10.1088/1674-1056/abea8f
Journal homepage: http://cpb.iphy.ac.cn; http://iopscience.iop.org/cpb

What follows is a list of articles you may be interested in

Opto-electromechanically induced transparency in a hybrid opto-electromechanical system

Hui Liu(刘慧), Li-Guo Qin(秦立国), Li-Jun Tian(田立君), Hong-Yang Ma(马鸿洋)
Chin. Phys. B, 2019, 28 (**10**): 108502. DOI: 10.1088/1674-1056/ab3af2

Efficient molecular model for squeeze-film damping in rarefied air

Cun-Hao Lu(陆存豪), Pu Li(李普), Yu-Ming Fang(方玉明)
Chin. Phys. B, 2019, 28 (**9**): 098501. DOI: 10.1088/1674-1056/ab3443

Electrically controlled optical switch in the hybrid opto-electromechanical system

Li-Guo Qin(秦立国), Zhong-Yang Wang(王中阳), Hong-Yang Ma(马鸿洋), Shu-Mei Wang(王淑梅), Shang-Qing Gong(龚尚庆)
Chin. Phys. B, 2017, 26 (**12**): 128502. DOI: 10.1088/1674-1056/26/12/128502

Excellent ethanol sensing properties based on Er_2O_3-Fe_2O_3 nanotubes

Liu Chang-Bai, He Ying, Wang Sheng-Lei
Chin. Phys. B, 2015, 24 (**11**): 118501. DOI: 10.1088/1674-1056/24/11/118501

Excellent acetone sensing properties of porous ZnO

Liu Chang-Bai, Liu Xing-Yi, Wang Sheng-Lei
Chin. Phys. B, 2015, 24 (**1**): 018503. DOI: 10.1088/1674-1056/24/1/018503

Reversible waveform conversion between microwave and optical fields in a hybrid opto-electromechanical system*

Li-Guo Qin(秦立国)[1,2], Zhong-Yang Wang(王中阳)[2,†], Jie-Hui Huang(黄接辉)[1], Li-Jun Tian(田立君)[3], and Shang-Qing Gong(龚尚庆)[4,‡]

[1] School of Mathematics, Physics and Statistics, Shanghai University of Engineering Science, Shanghai 201620, China
[2] Shanghai Advanced Research Institute, Chinese Academy of Sciences, Shanghai 201210, China
[3] Department of Physics, Shanghai University, Shanghai 200444, China
[4] Department of Physics, East China University of Science and Technology, Shanghai 200237, China

(Received 19 December 2020; revised manuscript received 27 January 2021; accepted manuscript online 1 March 2021)

We present a scheme of reversible waveform conversion between microwave and optical fields in the hybrid opto-electromechanical system. As an intermediate interface, nanomechanical resonator optomechanically couples both optomechanical cavities in the optical and microwave frequency domains. We find the double-optomechanically induced transparency and achieve coherent signal waveform bi-directional transfer between microwave and optical fields based on quantum interference. In addition, we give an analytical expression of one-to-one correspondence between the microwave field and the optical output field, which intuitively shows the reversible waveform conversion relationship. In particular, by numerical simulations and approximate expression, we demonstrate the conversion effects of the three waveforms and discuss the bi-directional conversion efficiency and the bandwidth. such a hybrid opto- and electro-mechanical device has significant potential functions for electro-optic modulation and waveform conversion of quantum microwave-optical field in optical communications and further quantum networks.

Keywords: opto-electromechanical systems, photoelectric conversion, cavity quantum electrodynamics, opto-electromechanically induced transparency

PACS: 85.85.+j, 84.60.Jt, 42.50.Pq, 42.15.Eq **DOI:** 10.1088/1674-1056/abea8f

1. Introduction

The efficient conversion of signals between the microwave at several gigahertz and the optical domain at hundreds of terahertz is a key technology in modern communication networks, especially in the connection between classical and quantum communication networks.[1–7] Over the past few decades, the information is processed electronically at microwave frequencies of several gigahertz.[2] Lots of engineered quantum systems in the microwave domain have been studied for quantum information processing, such as superconducting qubits and resonators,[8,9] electron spins of nitrogen–vacancy center in diamond,[10] and hyperfine states in ion trap qubits.[11] However, microwave frequency photons are difficult to transmit over long distances due to the thermal noise at the room temperature[8] and high loss $\sim$1 dBm^{-1} with the optimal microwave cables at 10 GHz.[3] Photons in optical domain show complementary features with the microwave photons, such as ultra low transmission loss in the fibres below 0.2 dBm^{-1} at telecom wavelength with the frequency 193 THz,[3] almost none thermal occupancy, highly efficient single-photon detectors, and long-lived quantum memories.[2] In addition, low decoherence and dissipation rates make optical photons as an ideal information carrier, which can be easily distributed between distant nodes in a quantum network via optical fibre and waveguide.[12,13] The disadvantage of the optical photon is the weak single-photon nonlinearity, which prevents the development of quantum gates.[14] These suggest the required techniques of bi-directional conversion of information between microwave and optical fields.

Such a converter with high-efficient conversion is useful to quantum information processing and quantum network.[2,3] The coherent conversion of photons has been proposed, including spin ensemble,[10,15] cavity quantum electrodynamics,[16] and the mechanical-membrane in electro-optomechanical systems.[1,7,17–20] Recent progresses including bi-directional operation,[21] coherent coupling,[22] and efficient conversion[23] make use of a mechanical oscillator as the transducer.

In cavity opto-electromechanical quantum system, a nanomechanical resonator (NMR) as a interface can couple a microwave device and an optical device on both sides of it. In such a hybrid device, we have reported a scheme of electro-optic waveform interconnect based on quantum interference.[24] In this work, we present a bi-directional con-

*Project supported by the National Natural Science Foundation of China (Grant Nos. 61605225, 11774089, 12034007，11664018, and 61772295) and the Natural Science Foundation of Shanghai, China (Grant No. 16ZR1448400).

†Corresponding author. E-mail: wangzy@sari.ac.cn
‡Corresponding author. E-mail: sqgong@ecust.edu.cn

© 2021 Chinese Physical Society and IOP Publishing Ltd

version between microwave and optical fields in a hybrid electro-optomechanical device. As an interface, the NMR bridges quantum linking between microwave and optical cavities in the wide different frequency domains. In the hybrid device, we can find that the single optomechanically induced transparency (OMIT)[25–28] in the optical frequency domain is split into double-OMIT due to adding the optomechanical coupling in the microwave frequency domain, *i.e.*, a new absorption peak appears in the OMIT window. The mechanism of double-OMIT is quantum interference with N-type energy-level from the coherent interaction of two kinds of photons and phonons in cavity optomechanics. By making use of this feature, we present a scheme of reversible waveform conversion between microwave and optical fields. The internal conversion efficiency in the device is determined by the microwave and optical cooperativities. The conversion bandwidth depends on the width of OMIT windows determined by the effective optomechanical coupling strength. Such a system can serve as a converter in hybrid quantum networks to connect optical and microwave fields.

Comparing with the other schemes, our model has the following advantages: (i) We obtain a bidirectional coherent conversion between the microwave and light signals, *i.e.*, reversible conversion. (ii) The conversion can be obtained in the two different or same frequency domains. (iii) The conversion waveform is arbitrary. (iv) The hybrid opto- and electromechanical system is simple and compact for the integration and application.

2. Model and method

As schematically shown in Fig. 1(a), our model consists of an optomechanical cavity (OMC) with the length l at an optical frequency $\omega_{\rm l}$ and a superconducting coplanar waveguide resonator (SCWR) that forms a microwave cavity with a microwave frequency ω_2. Two cavities share a common nanomechanical resonator (NMR) as a coupling interface, *i.e.*, the NMR not only acts as a mechanical mirror of the optical cavity, but also is capacitively coupled to the central conductor of SCWR. Therefore two kinds of cavities are symmetrical for NMR. Without loss of generality, we study the manipulation of the optical field by the microwave field as one example of interaction between the optical and microwave fields. The optomechanical system is driven by a strong coupling field with amplitude $\varepsilon_{\rm c}$ at frequency $\omega_{\rm c}$ and a weak probe field with amplitude $\varepsilon_{\rm p}$ at frequency $\omega_{\rm p}$. The microwave cavity can be described by the equivalent inductance L and capacitance $C+C(x)$ as shown in Fig. 1(b), and driven by the electric potential $e(t)=-{\rm i}\sqrt{2\hbar\omega_2 L}\varepsilon_{\rm in}({\rm e}^{-{\rm i}\omega_{\rm w}t}-{\rm e}^{{\rm i}\omega_{\rm w}t})$ with the frequency $\omega_{\rm w}$.[29] Under the common actions of radiation pressure forces arisen from the optical and microwave fields, the NMR will oscillate at near its equilibrium position with frequency $\omega_{\rm m}$. The displacement of the NMR changes the lengths of both cavities, simultaneously, *i.e.*, cavity resonance frequency. Here the displacement of the NMR from its equilibrium position is denoted by x, therefore, the effective OMC length will become $l+x$, then the resonance frequency is given as $\omega_{\rm l}(x)=\omega_{\rm l}(1-x/l)$. The coupling capacitance in the microwave cavity may be approximated by $C(x)=C_0(1+x/d)$ with the effective distance $d(x)=d-x$, where C_0 represents an equilibrium capacitance and d describes the distance between the equilibrium NMR and the central conductor of SCWR (*i.e.*, the plates of the capacitor in Fig. 1(b)), thus the microwave cavity has a total capacitance $C_{\rm total}=C(x)+C$ and frequency $\omega_2=1/\sqrt{LC_{\rm total}}$. Here we use the assumption $x\ll l,d$.

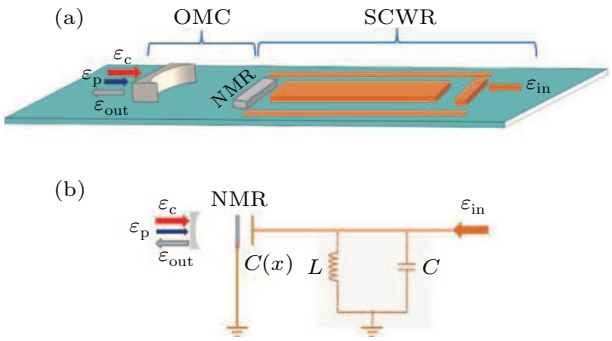


Fig. 1. Schematic diagram of reversible converter between microwave and optical fields in the hybrid of the opto-electromechanical system: (a) a nanomechanical resonator is coupled optomechanically to an optical cavity on the right and capacitively to a superconductig coplanar microwave cavity on the left, simultaneously; (b) equivalent circuit, where SCWR can be viewed as an LC oscillation circuit with the fixed inductance L and tunable capacitance as a sum of the constant capacitance C and the mechanically adjustable capacitance $C(x)$.

The total Hamiltonian of the system can be written as $H=H_{\rm fre}+H_{\rm int}+H_{\rm dri}$, which includes the free Hamiltonian $H_{\rm fre}$ of two cavities and the NMR, the interaction Hamiltonian $H_{\rm int}$ between NMR and two cavities, and the driven Hamiltonian $H_{\rm dri}$ of the two cavity-driven terms. Three Hamiltonians can be given respectively as

$$\begin{aligned}
H_{\rm fre} &= \hbar\omega_{\rm l}a^{\dagger}a+\hbar\omega_{\rm m}b^{\dagger}b+\hbar\omega_2 c^{\dagger}c,\\
H_{\rm int} &= -\hbar G_{\rm ab}a^{\dagger}a(b^{\dagger}+b)-\hbar G_{\rm bc}(c^{\dagger}c)(b^{\dagger}+b),\\
H_{\rm dri} &= {\rm i}\hbar\varepsilon_{\rm c}(a^{\dagger}{\rm e}^{-{\rm i}\omega_{\rm c}t}-a{\rm e}^{{\rm i}\omega_{\rm c}t})+{\rm i}\hbar\varepsilon_{\rm p}(a^{\dagger}{\rm e}^{-{\rm i}\omega_{\rm p}t}-a{\rm e}^{{\rm i}\omega_{\rm p}t})\\
&\quad +{\rm i}\hbar\varepsilon_{\rm in}(c^{\dagger}{\rm e}^{-{\rm i}\omega_{\rm w}t}-c{\rm e}^{{\rm i}\omega_{\rm w}t}),
\end{aligned}\tag{1}$$

where a and c are the annihilation operators for the optical and microwave cavities, b is the phonon annihilation operator of the NMR with the displacement $x=x_{\rm ZPF}(b+b^{\dagger})$, where $x_{\rm ZPF}=\sqrt{\hbar/2m\omega_{\rm m}}$ is the mechanical zero-point fluctuation of NMR with the mass m. The optomechanical coupling strength $G_{\rm ab}=g_{\rm ab}x_{\rm ZPF}$ (or $G_{\rm bc}=g_{\rm bc}x_{\rm ZPF}$) corresponds to the shift of the optical (or microwave) cavity frequency due to the mechanical motion, where $g_{\rm ab}=\omega_{\rm l}/l$, $g_{\rm bc}=\mu\omega_2/2d$,

and $\mu = C_0/C_{\text{total}}$. $\varepsilon_{\text{c}} = \sqrt{2P_{\text{c}}\kappa_1/\hbar\omega_{\text{c}}}$ and $\varepsilon_{\text{p}} = \sqrt{2P_{\text{p}}\kappa_1/\hbar\omega_{\text{p}}}$ are the amplitudes of a strong pump field with the power P_{c} and the weak probe field with the power P_{p} inside the OMC with the decay rate κ_1, respectively. A microwave source $e(t)$ with $\varepsilon_{\text{in}} = \sqrt{2P_{\text{m}}\kappa_2/\hbar\omega_{\text{w}}}$ and the power P_{m} is injected into the SCWR with the decay rate κ_2 by the RF field.

In the opto-electromechanical hybrid system, the resonant frequencies of the OMC and microwave cavity are usually much higher than the NMR's frequency under the current experimentally conditions, *i.e.*, $\omega_{\text{m}} \ll \omega_{1,2}$. Based on the rotating transformation, the total Hamiltonian can be rewritten as

$$\begin{aligned} H =\ & \hbar\Delta_1 a^\dagger a + \hbar\omega_{\text{m}} b^\dagger b + \hbar\Delta_2 c^\dagger c - \hbar G_{\text{ab}} a^\dagger a (b^\dagger + b) \\ & - \hbar G_{\text{bc}} c^\dagger c (b^\dagger + b) + \text{i}\hbar\varepsilon_{\text{c}}(a^\dagger - a) \\ & + \text{i}\hbar\varepsilon_{\text{p}}(a^\dagger \text{e}^{-\text{i}\Delta_{\text{pc}}t} - a e^{\text{i}\Delta_{\text{pc}}t}) + \text{i}\hbar\varepsilon_{\text{in}}(c^\dagger - c)), \end{aligned} \tag{2}$$

where $\Delta_1 = \omega_1 - \omega_{\text{c}}$, $\Delta_2 = \omega_2 - \omega_{\text{w}}$, and $\Delta_{\text{pc}} = \omega_{\text{p}} - \omega_{\text{c}}$. By introducing the dissipation and fluctuation noise terms, the dynamic equations of the system can be given by

$$\begin{aligned} \dot{a} =\ & -(\kappa_1 + \text{i}\Delta_1)a + \text{i}G_{\text{ab}}(b^\dagger + b)a + \varepsilon_{\text{c}} + \varepsilon_{\text{p}}\text{e}^{-\text{i}\Delta_{\text{pc}}t} \\ & + \sqrt{2\kappa_{1,\text{ex}}}a_{\text{in}}, \\ \dot{b} =\ & -(\gamma_{\text{m}}/2 + \text{i}\omega_{\text{m}})b + \text{i}G_{\text{ab}}a^\dagger a + \text{i}G_{\text{bc}}c^\dagger c + \sqrt{2\gamma_{\text{m}}}\xi, \\ \dot{c} =\ & -(\kappa_2 + \text{i}\Delta_2)c + \text{i}G_{\text{bc}}(b^\dagger + b)c + \varepsilon_{\text{in}} + \sqrt{2\kappa_{2,\text{ex}}}c_{\text{in}}, \end{aligned} \tag{3}$$

where $\kappa_i = \kappa_{i,\text{ex}} + \kappa_{i,\text{in}}$ $(i = 1,2)$. $\kappa_{i,\text{in}}$ and $\kappa_{i,\text{ex}}$ are the intrinsic and external loss rates of cavity mode i, respectively. The NMR with the damping rate γ_{m} is affected by a Brownian noise with zero mean value and the correlation function[30,31]

$$\begin{aligned} \langle \xi(t)\xi(t')\rangle =\ & \frac{\gamma_{\text{m}}}{\omega_{\text{m}}} \int \frac{\text{d}\omega}{2\pi} \text{e}^{-\text{i}\omega(t-t')} \omega \left[\coth\left(\frac{\hbar\omega}{2k_{\text{B}}T}\right) + 1\right] \\ \approx\ & \gamma_{\text{m}}(2\bar{n}+1)\Delta(t-t'), \end{aligned}$$

where k_{B} is the Boltzmann constant, T is the temperature of the reservoir of the nanomechanical oscillator and $\bar{n} = [\exp(\hbar\omega_{\text{m}}/k_{\text{B}}T) - 1]^{-1}$ is the mean thermal excitation number of the resonator. The cavity dynamics also depend on the cavity input noise a_{in} (c_{in}) with zero mean value.[32] Here, we are only interested in the mean response of the system, therefore the Heisenberg–Langevin noise operators can be reduced to their expectation values, *i.e.*, the quantum and thermal noise terms can be ignored.

In order to obtain the solutions of the Heisenberg–Langevin equations, we only care about in the linear response of the driven optomechanical system to the weak probe field. In the case of $|\varepsilon_{\text{p}}| \ll |\varepsilon_{\text{c}}|, |\varepsilon_{\text{in}}|$, the dynamical equations of the system can be linearized by assuming $O = O_{\text{s}} + \Delta O$ ($O = a, b$, and c),[33,34] *i.e.*, each operator of the system can be decomposed as the sum of its steady-state value O_{s} and a small fluctuation δO. By assuming $\varepsilon_{\text{p}} \to 0$ and setting all time derivatives to zero, the steady-state values of the system can be gotten from Eq. (3) as

$$\begin{aligned} a_{\text{s}} =\ & \frac{\varepsilon_{\text{c}}}{\kappa_1 + \text{i}\delta_1'}, \\ b_{\text{s}} =\ & \text{i}\frac{G_{\text{ab}}|a_{\text{s}}|^2 + G_{\text{bc}}|c_{\text{s}}|^2}{\gamma_{\text{m}}/2 + \text{i}\omega_{\text{m}}}, \\ c_{\text{s}} =\ & \frac{\varepsilon_{\text{in}}}{\kappa_2 + \text{i}\delta_2'}, \end{aligned}$$

where $\delta_1' = \Delta_1 - G_{\text{ab}}(b_{\text{s}}^* + b_{\text{s}})$ and $\delta_2' = \Delta_2 - G_{\text{bc}}(b_{\text{s}}^* + b_{\text{s}})$ are the effective detuning of the optical and microwave cavities due the motion of the NMR, respectively. By substituting $O = O_{\text{s}} + \delta O$ into Eq. (3) and ignoring high-order nonlinear terms, the Heisenberg–Langevin equations of ΔO are given by

$$\begin{aligned} \delta\dot{a} =\ & -(\kappa_1 + \text{i}\delta_1')\delta a + \text{i}G_{\text{abs}}(\delta b^\dagger + \delta b) + \varepsilon_{\text{p}}\text{e}^{-\text{i}\Delta_{\text{pc}}t}, \\ \delta\dot{b} =\ & -(\gamma_{\text{m}}/2 + \text{i}\omega_{\text{m}})\delta b + \text{i}(G_{\text{abs}}\delta a^\dagger + G_{\text{abs}}^*\delta a) \\ & + \text{i}(G_{\text{bcs}}\delta c^\dagger + G_{\text{bcs}}^*\delta c), \\ \delta\dot{c} =\ & -(\kappa_2 + \text{i}\delta_2')\delta c + \text{i}G_{\text{bcs}}(\delta b^\dagger + \delta b), \end{aligned} \tag{4}$$

where the effective coupling strength $G_{\text{abs}} = G_{\text{ab}}a_{\text{s}}$ and $G_{\text{bcs}} = G_{\text{bc}}c_{\text{s}}$ can be enhanced by the input fields. By introducing $\delta a = \delta\tilde{a}_+\text{e}^{-\text{i}\Delta_{\text{pc}}t}$, $\delta b = \delta\tilde{b}_+\text{e}^{-\text{i}\Delta_{\text{pc}}t}$, and $\delta c = \delta\tilde{c}_+\text{e}^{-\text{i}\Delta_{\text{pc}}t}$, we can ignore the fast oscillating terms $\text{e}^{\text{i}2\Delta_{\text{pc}}t}$ and get the following equations:

$$\begin{aligned} \delta\dot{\tilde{a}}_+ =\ & -(\kappa_1 - \text{i}\Delta_1')\delta\tilde{a}_+ + \text{i}G_{\text{abs}}\delta\tilde{b}_+ + \varepsilon_{\text{p}}, \\ \delta\dot{\tilde{b}}_+ =\ & -(\gamma_{\text{m}}/2 - \text{i}\Delta')\delta\tilde{b}_+ + \text{i}G_{\text{abs}}^*\delta\tilde{a}_+ + \text{i}G_{\text{bcs}}^*\delta\tilde{c}_+, \\ \delta\dot{\tilde{c}}_+ =\ & -(\kappa_2 - \text{i}\Delta_2')\delta\tilde{c}_+ + \text{i}G_{\text{bcs}}\delta\tilde{b}_+, \end{aligned} \tag{5}$$

where $\Delta_1' = \Delta_{\text{pc}} - \Delta_1'$, $\Delta_2' = \Delta_{\text{pc}} - \delta_2'$, and $\Delta' = \Delta_{\text{pc}} - \omega_{\text{m}}$. Under steady-state condition, we can obtain

$$\delta\tilde{a}_+ = \frac{\varepsilon_{\text{p}}}{\kappa_1 - \text{i}\Delta_1' + \dfrac{|G_{\text{abs}}|^2}{\gamma_{\text{m}}/2 - \text{i}\Delta' + \dfrac{|G_{\text{bcs}}|^2}{\kappa_2 - \text{i}\Delta_2'}}}. \tag{6}$$

In order to reveal the effects of the microwave field on the optical field, we will find out the response of the system to the probing frequency. By making use of the input–output relation of the cavity field in the rotating transformation $\varepsilon_{\text{out}} + \varepsilon_{\text{c}} + \varepsilon_{\text{p}}\text{e}^{-\text{i}\Delta_{\text{pc}}} = 2\kappa_1\langle a\rangle$, where $\varepsilon_{\text{out}} = \varepsilon_{\text{outs}} + \varepsilon_{\text{out}+}\text{e}^{-\text{i}\Delta_{\text{pc}}t}$ and $\langle a\rangle = a_{\text{s}} + \langle\delta\tilde{a}_+\rangle\text{e}^{-\text{i}\Delta_{\text{pc}}t}$, we can obtain $\varepsilon_{\text{out}} = \underbrace{(2\kappa a_{\text{s}} - \varepsilon_{\text{c}})}_{\text{Control field}} + \underbrace{(2\kappa\delta\tilde{a}_+ - \varepsilon_{\text{p}})\text{e}^{-\text{i}\Delta_{\text{pc}}t}}_{\text{Probe field}}$. We can see that the output field contains the input control field at the frequency ω_{c} and the probe field at the frequency ω_{p}. Therefore the output fields at the probe frequency yields $\varepsilon_{\text{out}+} = 2\kappa_1\delta\tilde{a}_+ - \varepsilon_{\text{p}}$.[35,36] For the modification of the probe field, we resort to the term ε_{T}, which is defined as

$$\varepsilon_{\text{T}} = \varepsilon_{\text{out}+}/\varepsilon_{\text{p}} + 1 = 2\kappa_1\delta\tilde{a}_+/\varepsilon_{\text{p}}. \tag{7}$$

The real and imaginary parts of $\varepsilon_{\rm T}$ show the absorption and dispersion of the OMC system, respectively.[25] After some simplification, we can rewrite the term of $\varepsilon_{\rm T}$ in a more intuitive relationship between the output probe field and the input microwave field as

$$\varepsilon_{\rm T} = \frac{2\kappa_1}{\kappa_1 - {\rm i}\Delta_1' + \dfrac{|G_{\rm abs}|^2}{\gamma_{\rm m}/2 - {\rm i}\Delta' + \dfrac{\left|\dfrac{G_{\rm bc}}{\kappa_2 + {\rm i}\delta_2'}\right|^2}{\kappa_2 - {\rm i}\Delta_2'}|\varepsilon_{\rm in}|^2}}. \tag{8}$$

3. Results and discussion

Now we investigate the conversion between the optical and microwave fields through NMR as an interface. To estimate the output field of OMC, the parameters are taken analogously to those of Refs. [29,37] for the NMR, that is, $m = 10$ ng, $\omega_{\rm m} = 2\pi \times 10.56$ MHz, $Q = 3.6 \times 10^4$, $\gamma_{\rm m} = \omega_{\rm m}/Q$, where Q is the quality factor of the NMR, for optical cavity of length $l = 1$ mm and damping rate $\kappa_1 = 0.08\omega_{\rm m}$, driven by a strong pump field with the wavelength $\lambda_{\rm c} = 810$ nm, for the microwave cavity with the frequency $\omega_{\rm w} = 7.19$ GHz, the damping rate $\kappa_2 = 0.01\omega_{\rm m}$, $\mu = 0.09$, and $d = 1.8$ nm.

As shown in Fig. 2, the absorption ${\rm Re}(\varepsilon_{\rm T})$ and dispersion ${\rm Im}(\varepsilon_{\rm T})$ of the output field are plotted as functions of $\Delta/\omega_{\rm m}$ for different powers of driven fields by setting $\Delta_1' = \Delta' = \Delta_2' = \Delta$, *i.e.*, the red detuning $\delta_1' = \delta_2' = \omega_{\rm m}$. We can find the OMIT windows from absent to single to double, which can be understood from the interference based on the level configuration in Fig. 3.[38] If the OMC is not driven by the strong pump field $\varepsilon_{\rm c}$, figure 2(a) shows the usual absorption and dispersion of the optical field with no transparency window. The output field becomes $\varepsilon_{\rm T} = 2k_1/(k_1 - {\rm i}\Delta)$, which only depends the OMC decay κ_1 and the detuning Δ. However, if the quality factor of the OMC is sufficiently high, the transparency can be opened up by the cavity vacuum, *i.e.*, the vacuum Rabi-splitting, which can lead to vacuum-induced transparency (VIT),[39] this case is not considered here. When the OMC is driven by the strong pump field and without the microwave field, the output field can be rewritten as

$$\varepsilon_{\rm T} = \frac{2k_1}{(k_1 - {\rm i}\Delta) + \dfrac{|G_{\rm abs}|^2}{\gamma_{\rm m}/2 - {\rm i}\Delta}}, \tag{9}$$

which has the standard form of OMIT due to the destructive interference between the probe field and the anti-Stokes field ($G_{\rm abs}$) generated by the pump pulse, as shown in Fig. 2(b). The width of the transparency window depends on the intensity of the effective coupling $|G_{\rm abs}|^2$ in the optical cavity, which can be adjusted by the input fields.[40]

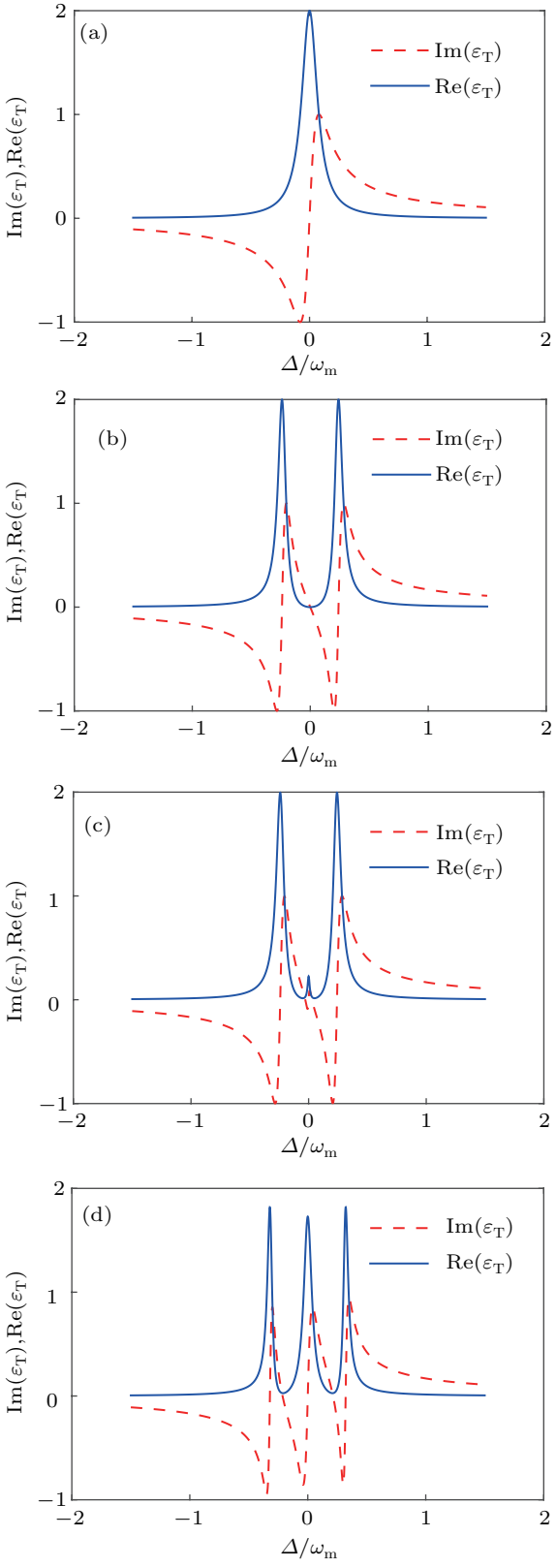


Fig. 2. The absorption ${\rm Re}(\varepsilon_{\rm T})$ (blue-solid line) and dispersion ${\rm Im}(\varepsilon_{\rm T})$ (red-dashed line) as a function of the detuning Δ in the different cases (a) $P_{\rm c} = 0$; (b) $P_{\rm c} = 60$ mW, $P_{\rm m} = 0$; (c) $P_{\rm c} = 60$ mW, $P_{\rm m} = 0.6$ μW; (d) $P_{\rm c} = 60$ mW, $P_{\rm m} = 24$ μW.

Further, when the optical and microwave fields interact simultaneously with NMR, the behavior of the probe output field becomes the double-OMIT,[36] which is caused by the additional coupled microwave field. Its real and imaginary

parts are shown in Figs. 2(c) and 2(d). A new absorption peak appears inside the transparency window in Fig. 2(b) due to the effect of the destructive interference.[38] The double-OMIT can be explained by the N-type energy level configuration in Fig. 3. When the NMR b is coupled to the microwave cavity c via the microwave optomechanical interaction, which is involved in the interference process, this microwave optomechanical interaction destroys the OMIT and splits one transparency window into two, *i.e.*, two dips appear as shown in Fig. 2(d). In addition, we can find that the middle new absorption peak become high as the power of microwave input field increases from Figs. 2(c) and 2(d).

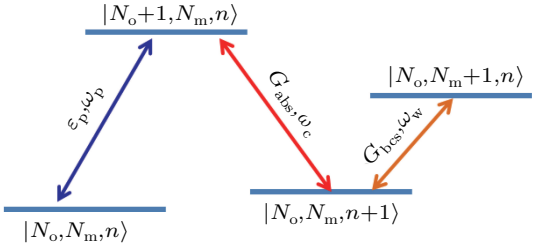


Fig. 3. Energy level structure of the simplified system. The number states of photons and phonons are denoted by $N_{o,m}$ and n, respectively. The effective optomechanical coupling strength between $|N_o+1,N_m,n\rangle$ and $|N_o,N_m,n+1\rangle$ in the optical domain is G_{abs}, and the effective optomechanical coupling strength between $|N_o,N_m,n+1\rangle$ and $|N_o,N_m+1,n\rangle$ is G_{bcs}.

When $\Delta = 0$ with the red detuning and the constant G_{abs}, we can construct the interconnection between microwave and optical fields and rewritten Eq. (8) as

$$\varepsilon_T = \frac{2\gamma_m\kappa_1\kappa_2 + 4\kappa_1|G_{bcs}|^2}{\gamma_m\kappa_1\kappa_2 + 2|G_{bcs}|^2\kappa_1 + 2|G_{abs}|^2\kappa_2}. \tag{10}$$

where $G_{bcs} = G_{bc}\varepsilon_{in}/(\kappa_2 + i\omega_m)$ is proportional to the input microwave field. Thus, we obtain an analytic expression of the relationship between the output field of OMC at the probe frequency and the input microwave field. Using this interconnect, we can generate an arbitrary waveform modulation of the optical field by adjusting the corresponding input microwave field. In the path, the input microwave field is transferred to the output of OMC along $\varepsilon_{in} \to c \to b \to a \to \varepsilon_T$, where the transmission amplitude is changed, but its waveform can be kept. To demonstrate the ability of the proposed scheme to transfer waveform between both different frequency signals, we give the numerical simulation results of Eq. (5) with $\Delta = 0$, the initial time $\delta\tilde{a}(0) = \delta\tilde{a}_s$, $\Delta\tilde{b}(0) = 0$, and $\delta\tilde{c}(0) = 0$, as shown in Fig. 4. For keeping high fidelity of the conversion from Eq. (10), the approximate conditions need be satisfied $\gamma_m\kappa_2 \ll 2|G_{bcs}|^2 \ll 2|G_{abs}|^2\kappa_2/\kappa_1$, *i.e.*, a high quality NMR and optical cavity. Further equation (10) can be approximatively rewritten as

$$\varepsilon_T = \frac{2\kappa_1}{\kappa_2} \cdot \frac{G_{bc}^2}{(\kappa_2^2 + \omega_m^2)|G_{abs}|^2} \cdot |\varepsilon_{in}|^2, \tag{11}$$

which is a one-to-one correspondence between the microwave field and the output probe field. Thus the waveform of the output probe field follows the waveform of the input microwave field, *i.e.*, a waveform conversion or interconnect.

For the transmission waveforms, we choose the standard and general cosine, square, and sawtooth waveforms as the input waveforms injected to SCWR, as shown by the solid lines in Figs. 4(a1), 4(b1), and 4(c1). Then, by using the numerical simulations, we obtain the corresponding transmission waveforms, indicated by the blue solid lines in Figs. 4(a2), 4(b2), and 4(c2). Based on Eq. (10), the corresponding analytic results of the output field are shown by the red dashed lines in Figs. 4(a2), 4(b2), and 4(c2). We can find that the envelopes of the simulation results are in good agreement with the waveforms of the analytical results, and approximatively follow the waveform of the input microwave field. The differences between both simulation and analytical results mainly originate from the transient process, which can not change the whole evolution envelope.

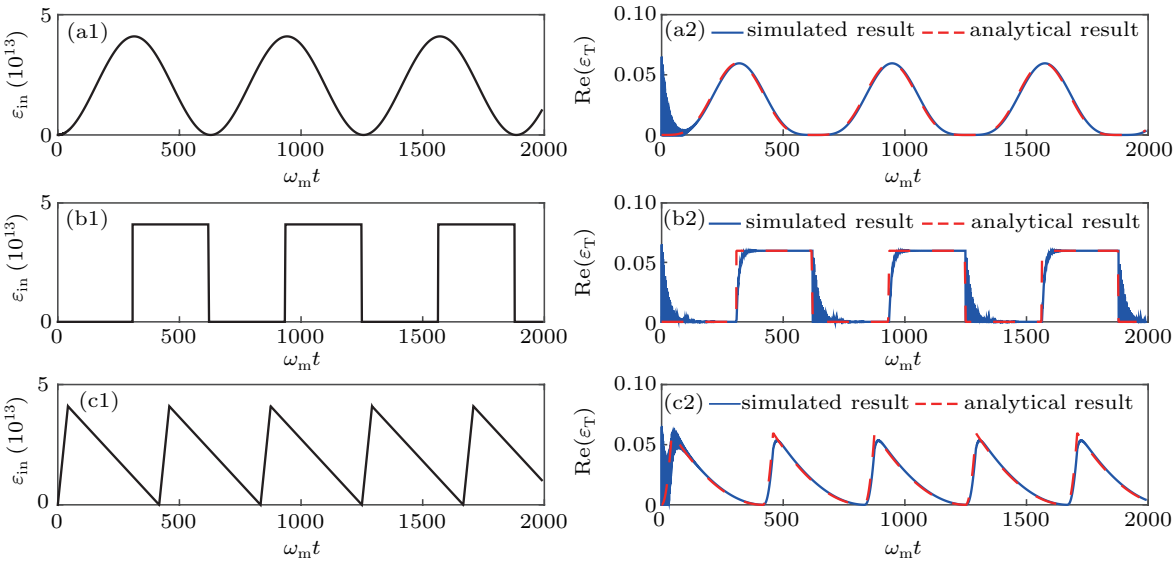


Fig. 4. Numerical and analytic results of the waveform conversion. Panels (a1), (b1), and (c1) show the input cosine, square, and sawtooth microwave waveforms injected into SCWR, and panels (a2), (b2), and (c2) show the numerical and analytic results of the cosine, square, and sawtooth waveform conversions, respectively. The other parameters are the same as those in Fig. 2(b).

In addition, if a strong control field and a weak probe field are injected into SCWR from the right side of the device, and a strong optical field is injected OMC from the left side of our device, that is, the positions of the mode a interchanges with that of the mode c in the total Hamiltonian of our system. From Eq. (1), we can see that the positions of a and c are symmetric in the Hamiltonians of before and after interchange positions of modes a and c, therefore the conversion waveform of optical to microwave frequency can be achieved based on the same method. Therefore, in this paper, we propose a feasible theoretical scheme for an arbitrary-waveform reversible conversion between microwave and optical wave. This scheme can be used to realize an arbitrary-waveform modulator between two fields in the different frequency domains.

To measure the conversion efficiency, we can use the conversion efficiency present by Tang.[8] To introduce the input and output of modes a and c into the equations of motion, we can give the reasonable assumptions including the resonance $\Delta = 0$, negligible the Brownian noise to NMR, the small cavity input $a_{\rm in}$ and $c_{\rm in}$. Then equation (5) can be rewritten as

$$\begin{aligned}
\delta\dot{\tilde{a}} &= -\kappa_1\delta\tilde{a} + {\rm i}G_{\rm abs}\delta\tilde{b} + \sqrt{2\kappa_{1,{\rm ex}}}a_{\rm in},\\
\delta\dot{\tilde{b}} &= -\gamma_{\rm m}/2\delta\tilde{b} + {\rm i}G^{*}_{\rm abs}\delta\tilde{a} + {\rm i}G^{*}_{\rm bcs}\delta\tilde{c},\\
\delta\dot{\tilde{c}} &= -\kappa_2\delta\tilde{c} + {\rm i}G_{\rm bcs}\delta\tilde{b} + \sqrt{2\kappa_{2,{\rm ex}}}c_{\rm in},\\
a_{\rm out} &= a_{\rm in} - \sqrt{2\kappa_{1,{\rm ex}}}\delta\tilde{a},\\
c_{\rm out} &= c_{\rm in} - \sqrt{2\kappa_{2,{\rm ex}}}\delta\tilde{c}.
\end{aligned} \tag{12}$$

By solving Eqs. (12) in the steady state case, we can get the relationship between the input and output of modes a and c as

$$\begin{pmatrix} a_{\rm out} \\ \\ c_{\rm out} \end{pmatrix} = \begin{pmatrix} 1 - \dfrac{2\lambda_3\sqrt{\kappa_{1,{\rm ex}}\kappa_{2,{\rm ex}}}}{\lambda_1\lambda_3 - |\lambda_2|^2} & -\dfrac{2\lambda_2\sqrt{\kappa_{1,{\rm ex}}\kappa_{2,{\rm ex}}}}{\lambda_1\lambda_3 - |\lambda_2|^2} \\ -\dfrac{2\lambda_2^{*}\sqrt{\kappa_{1,{\rm ex}}\kappa_{2,{\rm ex}}}}{\lambda_1\lambda_3 - |\lambda_2|^2} & 1 - \dfrac{2\lambda_1\sqrt{\kappa_{1,{\rm ex}}\kappa_{2,{\rm ex}}}}{\lambda_1\lambda_3 - |\lambda_2|^2} \end{pmatrix} \begin{pmatrix} a_{\rm in} \\ \\ c_{\rm in} \end{pmatrix},$$

where $\lambda_1 = \kappa_1 + \frac{|G_{\rm abs}|^2}{\gamma_{\rm m}/2}$, $\lambda_2 = \frac{G_{\rm abs}G^{*}_{\rm bcs}}{\gamma_{\rm m}/2}$, and $\lambda_3 = \kappa_2 + \frac{|G_{\rm bcs}|^2}{\gamma_{\rm m}/2}$. Thus, the bidirectional conversion efficiency can be written as

$$\eta = \left|\frac{a_{\rm out}}{c_{\rm in}}\right|^2 = \left|\frac{c_{\rm out}}{a_{\rm in}}\right|^2 = \frac{\kappa_{1,{\rm ex}}}{\kappa_1}\frac{\kappa_{2,{\rm ex}}}{\kappa_2} \times \frac{4C_1C_2}{(1+C_1+C_2)^2}, \tag{13}$$

where $C_1 = \frac{|G_{\rm abs}|^2}{\kappa_1\gamma_{\rm m}/2}$ and $C_2 = \frac{|G_{\rm bcs}|^2}{\kappa_2\gamma_{\rm m}/2}$ are defined as the optical mode a and microwave mode c cooperativities in the OMC and SCWR, respectively. As we can see from Eq. (13), the conversion efficiency consists of two parts: the system extraction efficiency which is $\eta_{\rm ex} = \frac{\kappa_{1,{\rm ex}}}{\kappa_1}\frac{\kappa_{2,{\rm ex}}}{\kappa_2}$, the internal conversion efficiency which is $\eta_{\rm in} = \frac{4C_1C_2}{(1+C_1+C_2)^2}$, *i.e.*, $\eta = \eta_{\rm ex} \times \eta_{\rm in}$. We can find that the internal conversion efficiency can never be larger than unity. Only when both cooperativities become larger, *i.e.*, $C_1, C_2 \gg 1$, will the internal conversion efficiency be greater and approaching 1, but not greater than 1. The conversion efficiency has the same form with the results given by Tang[8] and Li.[16]

From Figs. 2(c) and 2(d) and Eq. (8), we can find that the bandwidth of the output field at $\Delta = 0$ depends on the width of induced window, *i.e.*, the effective microwave-mechanical coupling strength $G_{\rm bcs}$ based on quantum interference. Therefore the bandwidth of the conversion is determined by the width of OMIT window depended on the effective optomechanical coupling strength $G_{\rm bcs}$, which can be modulated by the input microwave field and the quality factor of SCWR. When the waveform conversion from optical to microwaves is performed, and vice versa based on the same mechanism. For bidirectional conversion, the bandwidth of the conversion depends on both effective optomechanical coupling strengths $G_{\rm abs}$ and $G_{\rm bcs}$.

4. Conclusions

In summary, we proposed a scheme to realize a reversible optical to microwave waveforms conversion in two different frequency domains by a hybrid opto-electromechanical system based on quantum interference. The analytically convertive expression of one-to-one correspondence between the microwave field and the optical field has been given. The proposed scheme may built a bridge to interconnect two different frequency domains, *i.e.*, bi-directional waveform transfer. The internal conversion efficiency is determined by the microwave and optical cooperativities. The conversion bandwidth depends on the width of OMIT windows determined by the effective optomechanical coupling strength. It will be expanded into the field of information transmission and coding, linking low-loss transmission optical signals and deft microwave technologies to achieve complementary advantages of the microwave and optical waves. This scheme may have potential applications in future communication and signal processing systems.

References

[1] Andrews R W, Peterson R W, Purdy T P, Cicak K, Simmonds R W, Regal C A and Lehnert K W 2014 *Nat. Phys.* **10** 321
[2] Rueda A, Sedlmeir F, Collodo M C, Vogl U, Stiller B, Schunk G, Strekalov D V, Marquardt C, Fink J M, Painter O, Leuchs G and Schwefel H G L 2016 *Optica* **3** 597
[3] Lambert N J, Rueda A, Sedlmeir F and Schwefel H G L 2020 *Adv. Quantum. Technol.* **3** 1900077
[4] Jiang W, Sarabalis C J, Dahmani Y D, Patel R N, Mayor F M, McKenna T P, Laer R V and Safavi-Naeini A H 2020 *Nat. Commun.* **11** 1166
[5] Tian L 2015 *Ann. Phys.* **527** 1
[6] Wu M, Zeuthen E, Balram K C and Srinivasan K 2020 *Phys. Rev. Appl.* **13** 014027
[7] Jiang W, Sarabalis C J, Dahmani Y D, Patel R N, Mayor F M, McKenna T P, Laer R V and Safavi-Naeini A H 2020 *Nat. Commun.* **11** 1166
[8] Fan L, Zou C L, Cheng R, Guo X, Han X, Gong Z, Wang S and Tang H X 2018 *Sci. Adv.* **4** eaar4994
[9] Wendin G 2017 *Rep. Prog. Phys.* **80** 106001
[10] Marcos D, Wubs M, Taylor J M, Aguado R, Lukin M D and Sørensen A S 2010 *Phys. Rev. Lett.* **105** 210501
[11] Blatt R and Wineland D 2008 *Nature* **453** 1008
[12] O'Brien J L, Furusawa A and Vučković J 2009 *Nat. Photon.* **3** 687

[13] Lvovsky A I, Sanders B C and Tittel W 2009 *Nat. Photon.* **3** 706

[14] Kok P, Munro W J, Nemoto K, Ralph T C, Dowling J P and Milburn G J 2007 *Rev. Mod. Phys.* **79** 135

[15] Hafezi M, Kim Z, Rolston S L, Orozco L A, Lev B L and Taylor J M 2012 *Phys. Rev. A* **85** 020302

[16] Li J, Yu R and Wu Y 2014 *J. Appl. Phys.* **116** 164306

[17] Bagci T, Simonsen A, Schmid S, Villanueva L G, Zeuthen E, Appel J, Taylor J M, Sørensen A, Usami K, Schliesser A and Polzik E S 2014 *Nature* **507** 81

[18] Balram K C, Davanço M I, Song J D and Srinivasan K 2016 *Nat. Photon.* **10** 346

[19] Barzanjeh S, Abdi M, Milburn G J, Tombesi P and Vitali D 2012 *Phys. Rev. Lett.* **109** 130503

[20] Pei P, Huang H F, Guo Y Q, Zhang X Y and Dai J F 2018 *Chin. Phys. B* **27** 024203

[21] Vainsencher A, Satzinger K J, Peairs G A and Cleland A N 2016 *Appl. Phys. Lett.* **109** 033107

[22] Balram K C, Marcelo M I, Song J D and Srinivasan K 2016 *Nat. Photon.* **10** 346

[23] Higginbotham A P, Burns P S, Urmey M D, Peterson R W, Kampel N S, Brubaker B M, Smith G, Lehnert K W and Regal C A 2018 *Nat. Phys.* **14** 1038

[24] Qin L G, Wang Z Y, Gong S Q and Ma H Y 2017 *Photon. Res.* **5** 481

[25] Agarwal G S and Huang S 2010 *Phys. Rev. A* **81** 041803

[26] Weis S, Riviere R, Deleglise S, Gavartin E, Arcizet O, Schliesser A and Kippenberg T J 2010 *Science* **330** 1520

[27] Lu X H, Si L G, Wang B, Wang X Y and Wu Y 2019 *J. Phys. B: At. Mol. Opt. Phys.* **52** 085401

[28] Liu H, Qin L G, Tian L J and Ma H Y 2019 *Chin. Phys. B* **28** 108502

[29] Si L G, Guo L X, Xiong H and Wu Y 2018 *Phys. Rev. A* **97** 023805

[30] Giovannetti V and Vitali D 2001 *Phys. Rev. A* **63** 023812

[31] Benguria R and Kac M 1981 *Phys. Rev. Lett.* **46** 1

[32] Chakraborty S and Sarma A K 2018 *Phys. Rev. A* **97** 022336

[33] Jia W Z, Wei L F, Li Y and Liu Y 2015 *Phys. Rev. A* **91** 043843

[34] Feng L, You Y, Lin G, Niu Y and Gong S 2020 *Quantum. Inf. Process.* **19** 167

[35] Ma P C, Zhang J Q, Xiao Y, Feng M and Zhang Z M 2014 *Phys. Rev. A* **90** 043825

[36] Gu W J and Zhen Y 2014 *Opt. Commun.* **333** 261

[37] Teufel J D, Li D, Allman M S, Cicak K, Sirois A J, Whittaker J D and Simmonds R W 2011 *Nature* **471** 204

[38] Smith D D, Chang H, Fuller K A, Rosenberger A T and Boyd R W 2004 *Phys. Rev. A* **69** 063804

[39] Field J E 1993 *Phys. Rev. A* **47** 5064

[40] Javan A, Kocharovskaya O, Lee H and Scully M O 2002 *Phys. Rev. A* **66** 013805